Yuzuncu Yil University
Journal of the Institute of Natural & Applied Sciences

https://dergipark.org.tr/en/pub/yyufbed

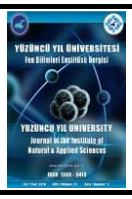

Research Article

Spectroscopic Characterizations and DFT Calculations of Olanzapine: Thermochemistry, HOMO-LUMO, FT-IR, MEP, and Hirshfeld Surface (HS) Analyses

Fermin AK*, Mehmet Hanifi KEBİROĞLU

Malatya Turgut Özal University, Darende Bekir Ilıcak Vocational School, Opticianry Program, 44700, Malatya, Türkiye
Fermin AK, ORCID No: 0000-0003-3238-4638,
Mehmet Hanifi KEBİROĞLU, ORCID No: 0000-0002-6764-3364
*Corresponding author e-mail: fermin.ak@ozal.edu.tr

Article Info

Received: 01.01.2024
Accepted: 10.07.2024
Online December 2024

DOI:10.53433/yyufbed.1413089

Keywords
FT-IR,
Hirshfeld surfaces,
HOMO and LUMO,
MEP,
Olanzapine,
Thermochemistry

Abstract: Olanzapine (OZ) was investigated quantum chemically using the Density Functional Theory (DFT) approach, and its surface was analyzed spectrochemically. To obtain the optimized structure, which serves as the basis for all other calculations, the LanL2DZ basis set was used. The DFT method has been employed to investigate the analysis of the title compound, specifically focusing on its ground state, which corresponds to the minimum energy state. The highest occupied molecular orbital (HOMO) and the lowest unoccupied molecular orbital (LUMO) energy levels of the frontier orbitals were obtained. The energy gap between HOMO and LUMO orbitals was determined to be 3.937 eV. HOMO-LUMO band gap (BG) emphasizes that adequate charge transfer has occurred within the molecule. In this context, Molecular Electrostatic Potential (MEP) surface analysis was investigated, and thermochemical properties of OZ ($C_{17}H_{20}N_4S$-molecular formula) were obtained and reported. The Hirshfeld surfaces including d_i, d_e, d_{norm}, shape index, curvedness, and fragment patch of $C_{17}H_{20}N_4S$ were pictured and discussed.

Olanzapinin Spektroskopik Karakterizasyonları ve DFT Hesaplamaları: Termokimya, HOMO-LUMO, FT-IR, MEP ve Hirshfeld Yüzey (HS) Analizleri

Makale Bilgileri

Geliş: 01.01.2024
Kabul: 10.07.2024
Online Aralık 2024

DOI:10.53433/yyufbed.1413089

Anahtar Kelimeler
FT-IR,
Hirshfeld yüzeyleri,
HOMO ve LUMO,
MEP,
Olanzapin,
Termokimya

Öz: Olanzapin (OZ), Yoğunluk Fonksiyonel Teorisi (DFT) yaklaşımı kullanılarak kuantum kimyasal olarak incelenmiş ve yüzeyi spektrokimyasal olarak analiz edilmiştir. Diğer tüm hesaplamalara temel teşkil eden optimize edilmiş yapıyı elde etmek için LanL2DZ temel seti kullanılmıştır. DFT metodu, minimum enerji durumuna karşılık gelen taban duruma özel olarak odaklanarak söz konusu bileşiğin analizini araştırmak için çalışılmıştır. Sınır yörüngelerin en yüksek dolu moleküler yörünge (HOMO) ve en düşük boş moleküler yörünge (LUMO) enerji seviyeleri elde edilmiştir. HOMO ve LUMO yörüngeleri arasındaki enerji aralığı 3.937 eV olarak belirlenmiştir. HOMO-LUMO bant aralığı (BG), molekül içerisinde yeterli yük aktarımının gerçekleştiğini vurgulamaktadır. Bu kapsamda, Moleküler Elektrostatik Potansiyel (MEP) yüzey analizi incelenmiş ve OZ'un ($C_{17}H_{20}N_4S$-moleküler formülü) termokimyasal özellikleri elde edilerek raporlanmıştır. $C_{17}H_{20}N_4S$'nin d_i, d_e, d_{norm}, şekil indeksi, kavisliliği ve parça yamasını içeren Hirshfeld yüzeyleri resmedilmiş ve tartışılmıştır.

1. Introduction

Olanzapine (OZ), known by its generic name $C_{17}H_{20}N_4S$, is an antipsychotic agent characterized by its molecular structure, which comprises three fused rings (phenyl, diazepine, and thiophene) and an N-methyl-piperazine substituent. The illustration in Figure 1 represents a unit cell drawing of OZ, which was generated using the VESTA program. Most crystalline forms of OZ primarily consist of the centrosymmetric dimer as their supramolecular building unit (Surampudi et al., 2020). Two OZ molecules combine to create a centrosymmetric dimer through intermolecular C-H/π interactions (Thakuria & Nangia, 2011). These dimer molecules closely pack on their concave surfaces, facilitating multiple interactions. The stability of the dimer is such that it can even be observed within mesoscopic solute-rich clusters (Surampudi et al., 2020).

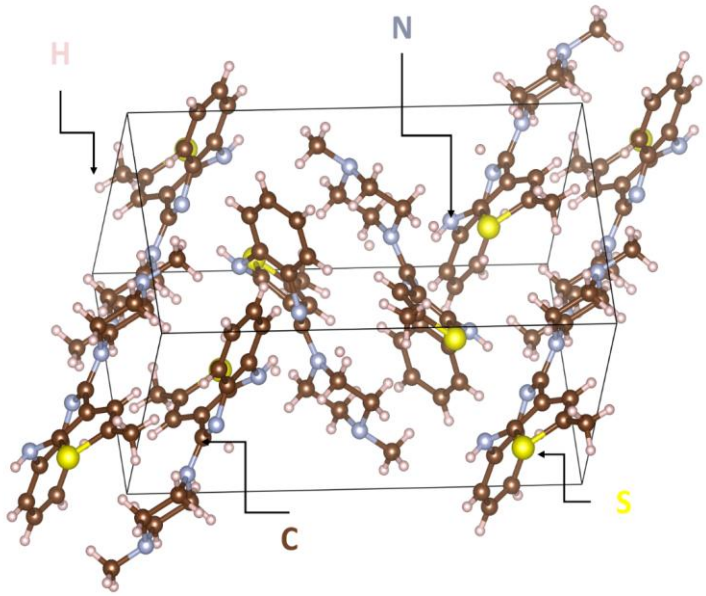

Figure 1. The packing arrangement of OZ molecules.

OZ (Olanzapine, 2-Methyl-4-(4-methyl-1-piperazinyl)- 10*H*-thieno[2,3-b][1,5]benzodiazepine (Sigmaaldrich, 2023) belongs to the class of newer generation atypical antipsychotic medications and is available in tablet form (Jasińska et al., 2009). Piperazine and thienobenzodiazepine derivatives find applications as antipsychotic, antidepressant, anti-inflammatory, antibiotic, antifungal, antimuscarinic agents, and antidiabetic, as well as in agrochemicals (Sevvanthi et al., 2020). OZ has also become the preferred therapeutic option for managing schizophrenia and acute mania in individuals with bipolar disorders (Paghandeh & Saeidian, 2018; Surampudi et al., 2020; Paghandeh et al., 2021). It is an antipsychotic medication (Surampudi et al., 2020). It, as a thienobenzodiazepine derivative (Bhana et al., 2001), also exhibits affinity for multiple neurotransmitter receptors. In vitro, it demonstrates substantial inhibitory activity at receptors for dopamine (D_1, D_2, D_4), serotonin (5-hydroxytryptamine; 5-HT) 5-HT_{2A}, 5-HT_{2C}, and histamine H_1 (Fulton & Goa, 1997).

Over the last three decades, OZ has gained popularity as a valuable tool compound for advancing our understanding of solid-state structure, form diversity, and crystallization outcomes at the molecular level, thanks to its remarkable solid-state chemistry, much like in physics (Reutzel-Edens & Bhardwaj, 2020). Computational chemistry suggests that antipsychotic drugs can be categorized based on their electron donor-acceptor capacity. Organic compounds have specific molecular orbitals, including the highest occupied molecular orbital (HOMO) and lowest unoccupied molecular orbitals (LUMO), which play a key role in chemical reactions. A higher HOMO energy in one compound can donate electrons to the LUMO energy in another, acting as an antioxidant. Conversely, a lower LUMO energy in one compound can accept electrons from the HOMO energy in another, acting as a prooxidant (Ozaki et al., 2023). The effects of this molecule on the body were identified using molecular docking studies (Al-Otaibi et al., 2021).

In this study, we employed Density Functional Theory (DFT) with the B3LYP functional and the LanL2DZ basis set to calculate excitation energies and other electronic properties (Beck, 1993). This method was chosen due to its proven accuracy in predicting the electronic structure of large molecules and its efficiency in handling systems involving heavy atoms (Hay & Wadt, 1985). The novelty of combining experimental and theoretical approaches allows for a comprehensive understanding of the material properties, providing insights that are benchmarked against experimental data to ensure reliability. Such theoretical studies are crucial for saving time and resources and for optimizing experimental procedures, starting with the determination of the most suitable molecular geometry where no negative vibrational frequencies are present (Cramer, 2013). In this research, we reported the results of DFT computations, which is a commonly used method for studying chemical reactivity (Frau et al., 2017). To enhance the accuracy of the theoretical results, excitation energies were computed using the LanL2DZ basis sets of the B3LYP functional, and the outcomes were compared (Tanış, 2022a). Gaussian 09 software, utilizing the LanL2DZ basis set, was employed for the theoretical calculations related to molecular structure and spectroscopy. These theoretical studies are crucial for saving time and resources and for optimizing experimental procedures. The optimization process starts with identifying the most appropriate geometry where the molecule exhibits no negative vibrational frequencies (Tanış, 2022b).

The CIF file for OZ was retrieved from the Crystallography Open Database website (Crystallography, 2023). The focus of the research was to investigate related characterization methods for OZ.

2. Material and Methods

Density Functional Theory (DFT) stands as a quantum mechanical framework employed for the computation of properties within systems containing multiple electrons. This theory is extensively utilized in the analysis of electronic structures, molecular dynamics, and the prediction of diverse material characteristics. DFT serves as a robust tool for comprehending and foreseeing the intricate behaviors of electrons in complex systems, establishing itself as a fundamental approach in computational quantum chemistry and condensed matter physics. The basic idea of DFT is to characterize the electron density of the system with a single function that determines the total energy of the system. This makes it possible to calculate the properties of the system without having to calculate the wave function of the system directly (Marques & Gross, 2004).

As seen in Table 1, the DFT method and LanL2DZ basis set were selected for having the most ideal energy gaps between the HOMO-LUMO orbitals among the sets. The LanL2DZ basis set, a double zeta (DZ) basis set, was developed by Hay and Wadt at the Los Alamos National Laboratory. It is a contracted basis set, so some of the basis functions are combined to reduce the number of basis functions without significantly affecting the accuracy of the calculation. The LanL2DZ basis set is a popular choice for DFT calculations of molecules and materials. It is relatively inexpensive to compute while still providing good accuracy for many properties (Chiodo et al., 2006).

Table 1. The energy gap between HOMO-LUMO orbitals of sets

Basis Sets	DFT (eV)	HF (eV)
STO-3G	4.463	11.795
3-21G	3.990	10.292
6-31G	3.962	10.197
6-311G	4.002	10.173
LanL2DZ	3.937	10.134
LanL2MB	4.263	11.661
SDD	3.950	10.156

Hirshfeld Surface (HS) Analysis was used to determine intramolecular and intermolecular connections and H-linked interactions within the crystal surface of a molecule. It is the most effective method for analyzing the unit cell arrangement of crystals. The OZ molecule has been utilized for the qualitative and quantitative examination of crystals, featuring a three-dimensional graphical

representation of the geographic area where nearby atoms interact and a two-dimensional fingerprint that identifies the atomic interactions (Hirshfeld, 1977; Wang et al., 2016). Crystal Explorer 17 software was used to register the Hirshfeld surface and fingerprint. It is used to analyze interactions within the crystal. Hirshfeld surface images are represented as d_{norm}. The d_i and d_e tips in the two-dimensional fingerprint diagram express the intermolecular interactions that exist within the molecules of the crystal (Hirshfeld, 1977; Kawahata et al., 2020).

3. Results

3.1. Geometry optimization

Geometry optimization involves seeking to determine the configuration with the lowest possible energy of a molecule. From a technical perspective, it estimates the wave function and energy in the initial geometry before searching for the geometry with the lowest energy. Optimizations produced through DFT and HF techniques within the scope of the LanL2DZ basis set are considered suitable, as outlined in Table 1. Fine-tuned parameters such as bond angles and bond lengths, determined using various techniques like DFT and HF, exhibit strong agreement with the corresponding X-ray structural characteristics, with only minor variations in the numerical values (Khanum et al., 2022). Figure 2 represents the optimized structure visually.

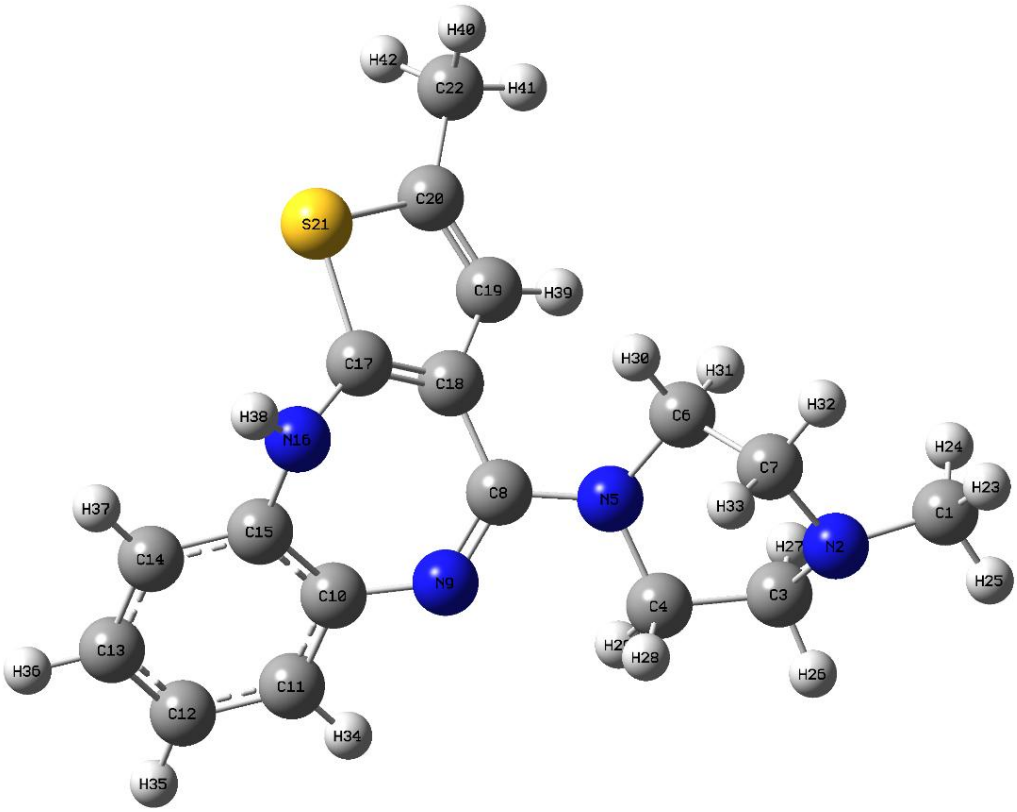

Figure 2. Optimized structure of OZ.

3.2. Natural Bond Orbital (NBO) analysis

NBO analysis gives complete orbital information about electronic density. It shows the inside of the molecule and the interactions between molecules (Eryilmaz et al., 2017). Additionally, it provides insight into the electron distributions in the subshells of atomic orbitals (Ulaş, 2020). C17-S21 has the longest tie length and is 1.8319 Å. The S atom remains distant from binding to the molecule. In Figure 3, the Color Range is between 1.013 - 1.832. The reason the colors are green shows that the distance between the atom and the molecule is long. The bond length of C-C bond values ranges from 1.346–1.516 A˚ for OZ. In the OZ compound, the C-H bond ranges from 1.084–1.108 A˚ (Sevvanthi et al.,

2020). The initial parameters for NBO analysis can be found in Table 2, which details Electronic Density and Bond Lengths.

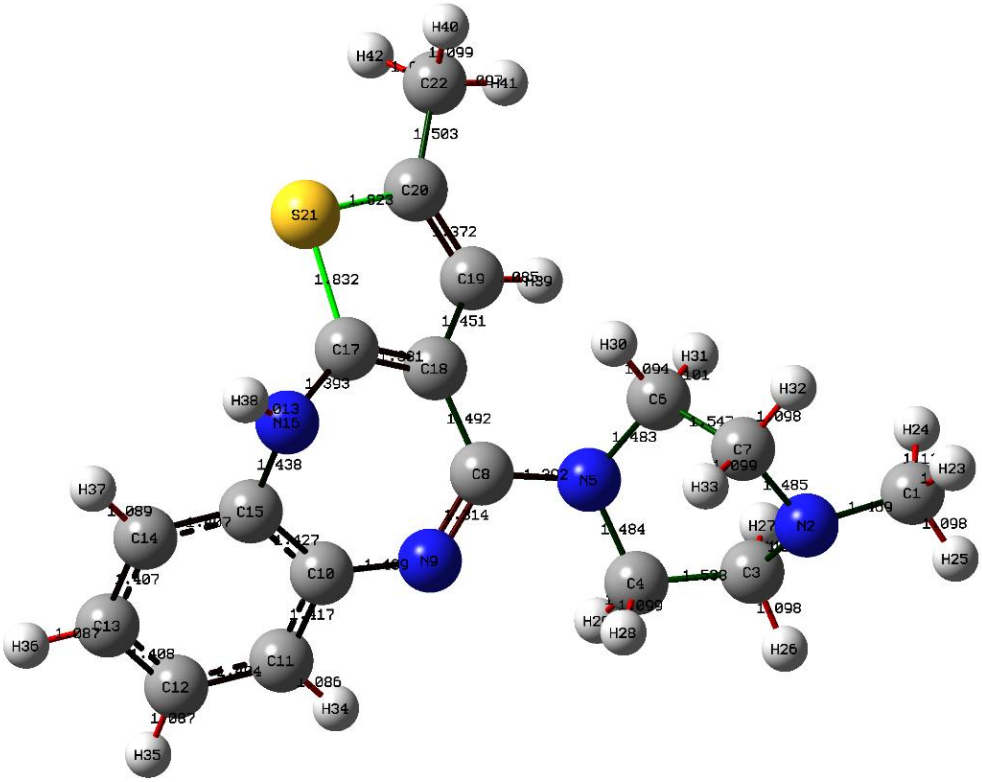

Figure 3. Bond Lengths (Color Range 1.013 to 1.832).

Table 2. Initial Parameters for OZ

Definition	Value (Å)	Definition	Value(Å)
C1-N2	1.4693	C10-C15	1.4274
C1-H23	1.0962	C11-C12	1.4038
C1-H24	1.1115	C11-H34	1.0862
C1-H25	1.0977	C12-C13	1.4084
N2-C3	1.4808	C12-H35	1.0873
N2-C7	1.4854	C13-C14	1.4066
C3-C4	1.5335	C13-H36	1.087
C3-H26	1.0985	C14-C15	1.4074
C3-H27	1.1111	C14-H37	1.089
C4-N5	1.4835	C15-N16	1.4378
C4-H28	1.0994	N16-C17	1.393
C4-H29	1.0944	N16-H38	1.0129
N5-C6	1.483	C17-C18	1.3807
N5-C8	1.3916	C17-S21	1.8319
C6-C7	1.5472	C18-C19	1.4508
C6-H30	1.0937	C19-C20	1.3717
C6-H31	1.1011	C19-H39	1.0849
C7-H32	1.0979	C20-S21	1.8233
C7-H33	1.0995	C20-C22	1.5029
C8-N9	1.3138	C22-H40	1.0987
C8-C18	1.4917	C22-H41	1.0967
N9-C10	1.4092	C22-H42	1.0982
C10-C11	1.4171		

3.3. Frontier Molecular Orbital (FMO) analysis

The frontier molecular orbitals, specifically HOMO and LUMO, along with the energy gap between these orbitals, play a crucial role in determining electronic and optical properties (Tanış, 2022c). The band gap value is determined by the energy difference between the frontier orbital levels of HOMO and LUMO (Tanış, 2022d). The computed frontier energy gap between HOMO and LUMO energies at the DFT/LanL2DZ level for OZ is shown in Figure 4. Figure 4 shows the molecular orbital arrangement and energy state diagram of OZ. The value of HOMO is -4.959 eV, and LUMO is -1.022 eV. The energy gap for OZ is 3.937 eV. The global hardness (η) of 1.968 eV, the chemical potential (μ) of -2.990 eV, and the global electrophilicity power (ω) of 2.271 eV is calculated for the OZ from the values of HOMO and LUMO. The parameter formulas used for these are shown below (Çakmak et al., 2022). Quantum chemical descriptors calculated for OZ are listed in Table 3.

$$I = -E_{HOMO} \tag{1}$$

$$A = -E_{LUMO} \tag{2}$$

$$\eta = \frac{1}{2}\left[\frac{\partial^2 E}{\partial^2 N}\right]_{v(r)} = \frac{I - A}{2} \tag{3}$$

$$\langle \alpha \rangle = \frac{1}{3}\left[\alpha_{xx} + \alpha_{yy} + \alpha_{zz}\right] = \sigma = \frac{1}{\eta} \tag{4}$$

$$\mu = -\chi = \left[\frac{\partial E}{\partial N}\right]_{V(r)} = -\left(\frac{I + A}{2}\right) \tag{5}$$

$$\omega = \frac{\chi^2}{2\eta} \tag{6}$$

$$\varepsilon = \frac{1}{\omega} \tag{7}$$

$$\omega^{+} = \frac{(I + 3A)^2}{16(I - A)} \tag{8}$$

$$\omega^{-} = \frac{(3I + A)^2}{16(I - A)} \tag{9}$$

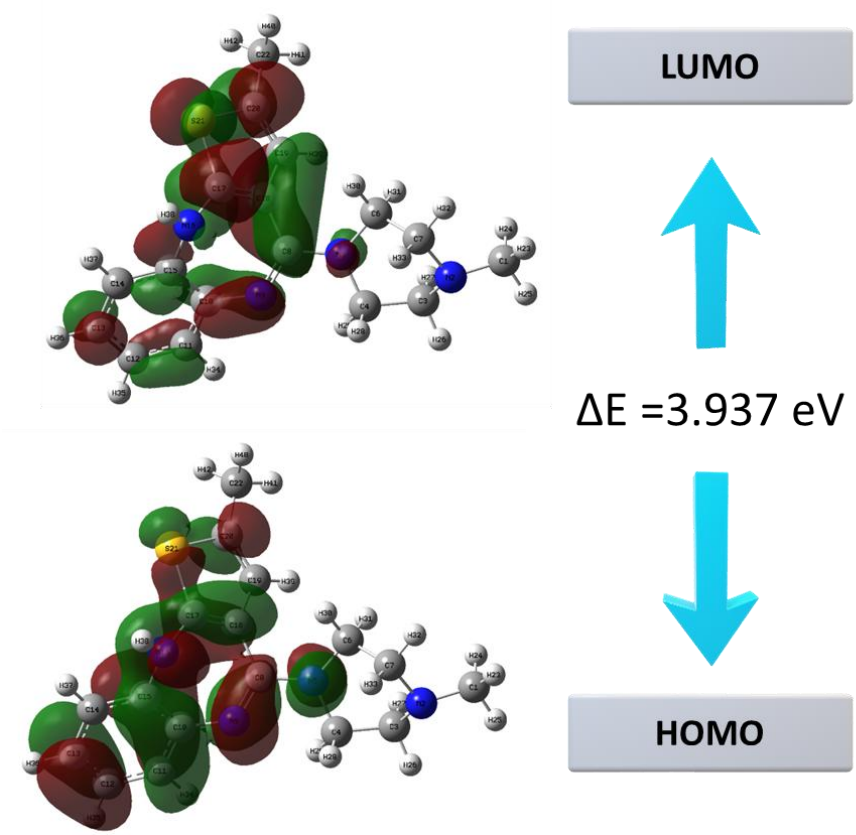

Figure 4. The molecular orbital arrangement and energy state diagram of OZ.

Table 3. The calculated quantum chemical descriptors for OZ

Parameter	Values	Parameter	Values
E_{HOMO} (eV)	-4.959	μ (eV)	-2.990
E_{LUMO} (eV)	-1.022	ω	2.271
ΔE (eV)	3.937	ε	0.440
η (eV)	1.968	ω^{+}	1.022
σ (eV^{-1})	0.508	ω^{-}	4.012
χ (eV)	2.990		

3.4. FT-IR spectra

The FT-IR spectra of OZ using the DTF/LanL2DZ set are shown in Figure 5. The high-frequency peaks in the IR spectrum are assigned to C1-H24 vibrations at 2915.66 cm^{-1} to 3074.51 cm^{-1}. The wavenumbers of these high-frequency peaks correspond to possible positions based on structural data. C1-H24 group vibrations are probably the most sensitive to the environment, thus showing marked changes in the spectra of hydrogen-bonded species. There are out-of-plane (at below 1000 cm^{-1}), stretching (sharp strong peaks) and in-plane bending (sharp weak to medium intensity bands) vibrations. In the present research, the strong Fourier transform infrared (FTIR) spectroscopy bands at 3074.51 cm^{-1} were assigned to C1-H24 stretching vibrations of OZ molecules. The N9-C8-C18-C17 stretching wavenumber can be easily recognized as the peak at 1641.87 cm^{-1} in the IR spectra, hence assigned to the stretching vibration (Alam & Lee, 2017; Devi et al., 2018).

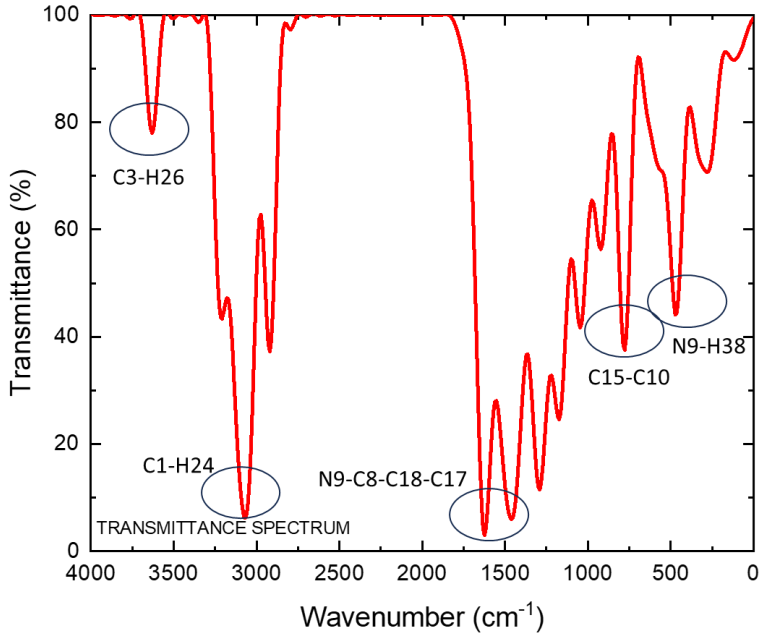

Figure 5. FT-IR spectrum of OZ.

3.5. MEP and Thermochemistry

The Molecular Electrostatic Potential (MEP) reveals the distribution of electronic density in a molecule, which proves valuable in identifying sites susceptible to electrophilic attacks, nucleophilic reactions, and hydrogen bonding interactions. MEP can highlight regions of a molecule that are electron-rich and thus more likely to attract electrophiles (electron-deficient species). These regions typically appear as areas of negative potential in the MEP map. Conversely, regions of a molecule that are electron-poor (positive potential) can attract nucleophiles (electron-rich species). These areas are essential for predicting sites where nucleophilic reactions are likely to occur (Kebiroğlu & Ak, 2023). The regions colored in red (N9 and N2 atoms) indicate negative areas, signifying a predisposition to electrophilic reactivity, while those in blue (N16 atom) denote positive areas, indicating a propensity for nucleophilic reactivity as illustrated in Figure 6a. A higher value of the electrophilicity index indicates a greater capacity of the molecule to accept electrons (Sheikhi et al., 2016). The equations used to calculate thermochemical data in Gaussian provide to obtain properties related to thermodynamics, as in Figure 6b (Ochterski, 2000).

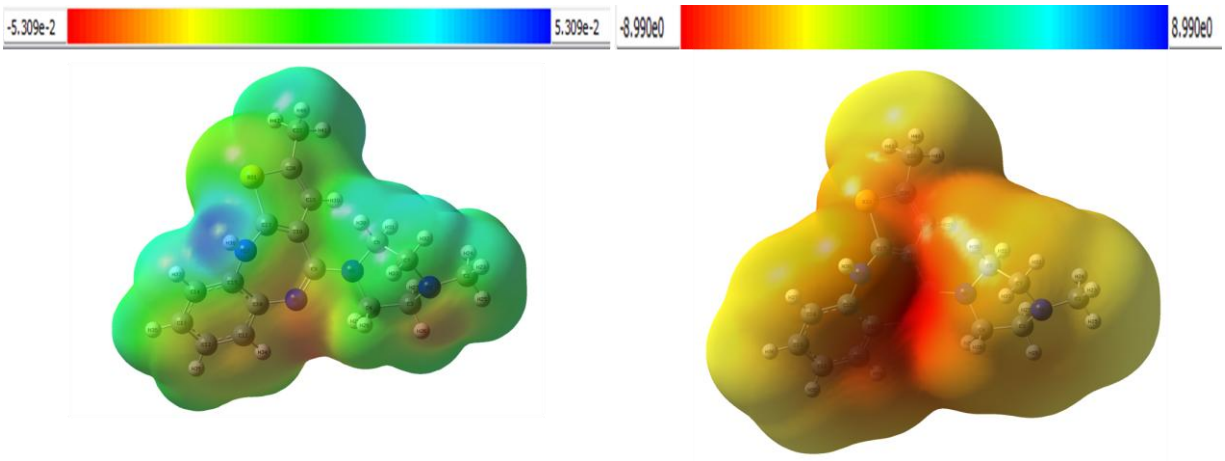

Figure 6. a) The 2D contour map of Molecular Electrostatic Potential (MEP) and b) ThermoChemistry Surface Map (TCSM) of OZ.

Because of the thermochemistry calculation of the molecule in Figure 6b, the temperature corresponds to the middle part of the molecule, namely the C8 atom. This is due to the central bonding of the C8 atom to the N5, N9, and C18 atoms, causing excessive heat to occur. The temperature was measured as 298.15 Kelvin and the pressure was measured as 1 atm. Furthermore, it was obtained that Thermo Chemistry Surface Maps (TCSM) of OZ is the same from 100 K to 350 K according to Figure 7. It shows that the structure is durable. The calculations for E (thermal), C_V (heat capacity), and S (entropy) parameters of OZ were in Table 4 and graphically represented as a correlation in Figure 8.

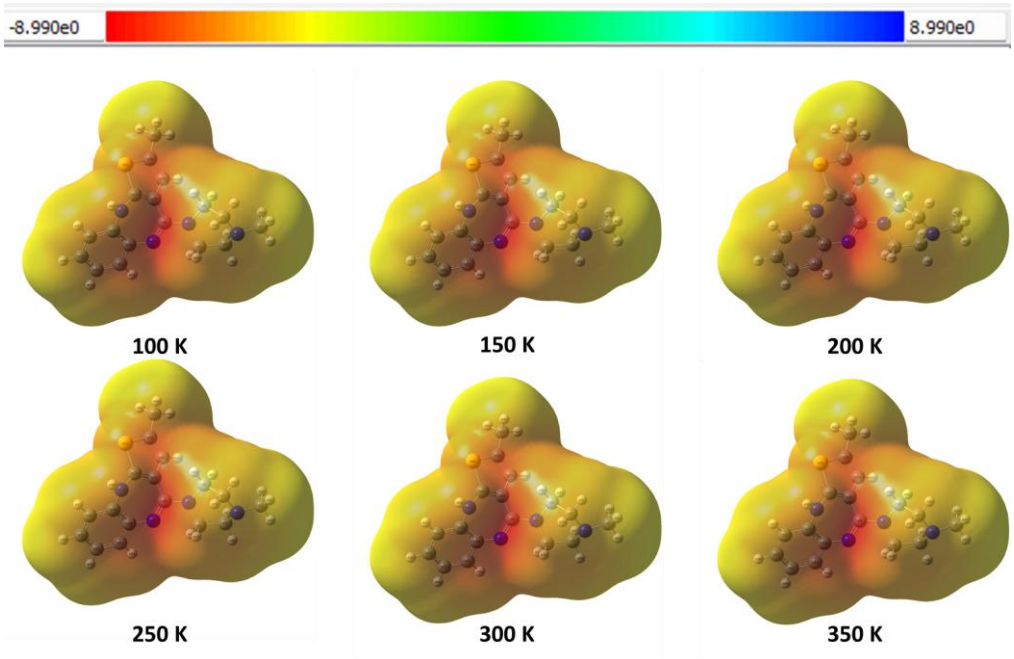

Figure 7. ThermoChemistry Surface Maps (TCSM) of OZ.

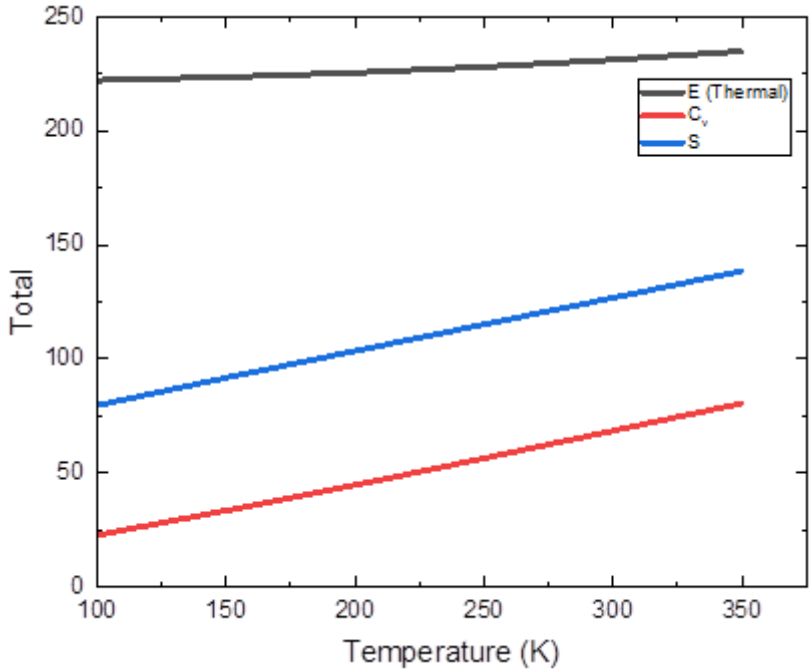

Figure 8. Theoretical thermal investigation as a correlation of E (thermal) energy, C_V (heat capacity), and S (entropy).

Table 4. Calculation of parameters of E (thermal), C_V (heat capacity), and S (entropy) of OZ

	Total			Translational			Rotational			Vibrational		
Temperature (K)	E (Thermal) (kcal/Mol)	C_V (Cal/Mol-K)	S (Cal/Mol-K)	E (Thermal) (kcal/Mol)	C_V (Cal/Mol-K)	S (Cal/Mol-K)	E (Thermal) (kcal/Mol)	C_V (Cal/Mol-K)	S (Cal/Mol-K)	E (Thermal) (kcal/Mol)	C_V (Cal/Mol-K)	S (Cal/Mol-K)
100	222.194	22.808	79.672	0.298	2.981	37.684	0.298	2.981	31.686	221.598	16.847	10.303
150	223.600	33.519	91.737	0.447	2.981	39.698	0.447	2.981	32.894	222.706	27.558	19.145
200	225.553	44.682	103.468	0.596	2.981	41.127	0.596	2.981	33.752	224.361	38.720	28.589
250	228.078	56.417	115.132	0.745	2.981	42.236	0.745	2.981	34.417	226.588	50.455	38.479
300	231.201	68.543	126.849	0.894	2.981	43.142	0.894	2.981	34.960	229.413	62.581	48.747
350	234.931	80.602	138.631	1.043	2.981	43.908	1.043	2.981	35.420	232.845	74.641	59.304

3.6. Hirshfeld Surface (HS) analysis

The Hirshfeld surface analysis methodology is employed for comprehending intermolecular interactions, identifying atoms in close contact, assessing crystal packing, and analyzing internuclear distances and angles (Spackman & Jayatilaka, 2009). This analytical method, through Hirshfeld surface analysis, offers a valuable graphical representation of hydrogen bond interactions. The Hirshfeld surface and fingerprint plots serve as useful tools for gaining insights into the contributions of interatomic contacts and assessing the stability of the molecular structure (Spackman & McKinnon, 2002). Hirshfeld surface images are represented as d_{norm}; while the red colored area indicates the negative d_{norm} side and close intermolecular interaction. The blue color area represents the longer intermolecular relationship and the positive d_{norm}. The zero-norm value is represented by the white part (Hirshfeld, 1977).

The red circular dot precipitated on the d_{norm} surface of the OZ structure represents intermolecular interactions. Negative d_{norm} values in surface regions indicate that the sum of d_i and d_e is shorter than the sum of the respective van der Waals radii (r_{vdw}) considered as the closest contact. This represents the normalized contact surface distance of the d_{norm} values and $d_i$and the internuclear distance. Figure 9 shows the Hirshfeld surface for OZ with d_i, d_e, d_{norm} shape index, curvature, and patch. Table 5 displays the distances related to Surface Feature Rescaling of OZ (Arulraj et al., 2020).

Table 5. Rescale Surface Property for OZ

Hirshfeld Surfaces	Rescale Surface	Property (Å)
d_{norm}	-0.3017	1.7049
d_i	0.9262	2.9282
d_e	0.9243	2.8423
Shape Index	-1.0000	1.0000
Curedness	-4.0000	0.4000
Fragment Patch	0.0000	16.0000

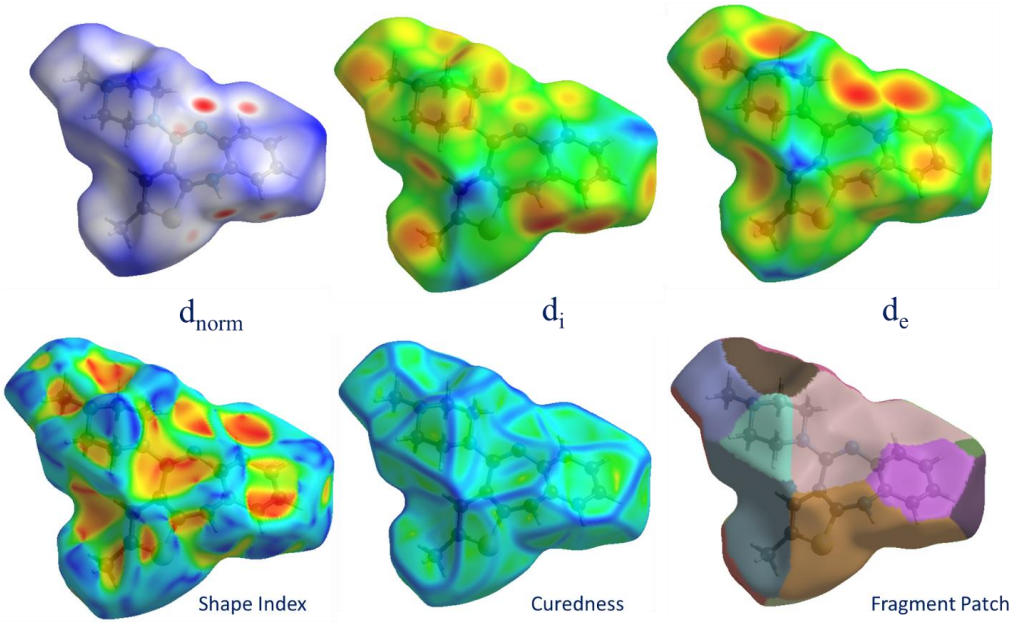

Figure 9. Hirshfeld surface for OZ with d_i, d_e, d_{norm}, shape index, curvedness and fragment patch.

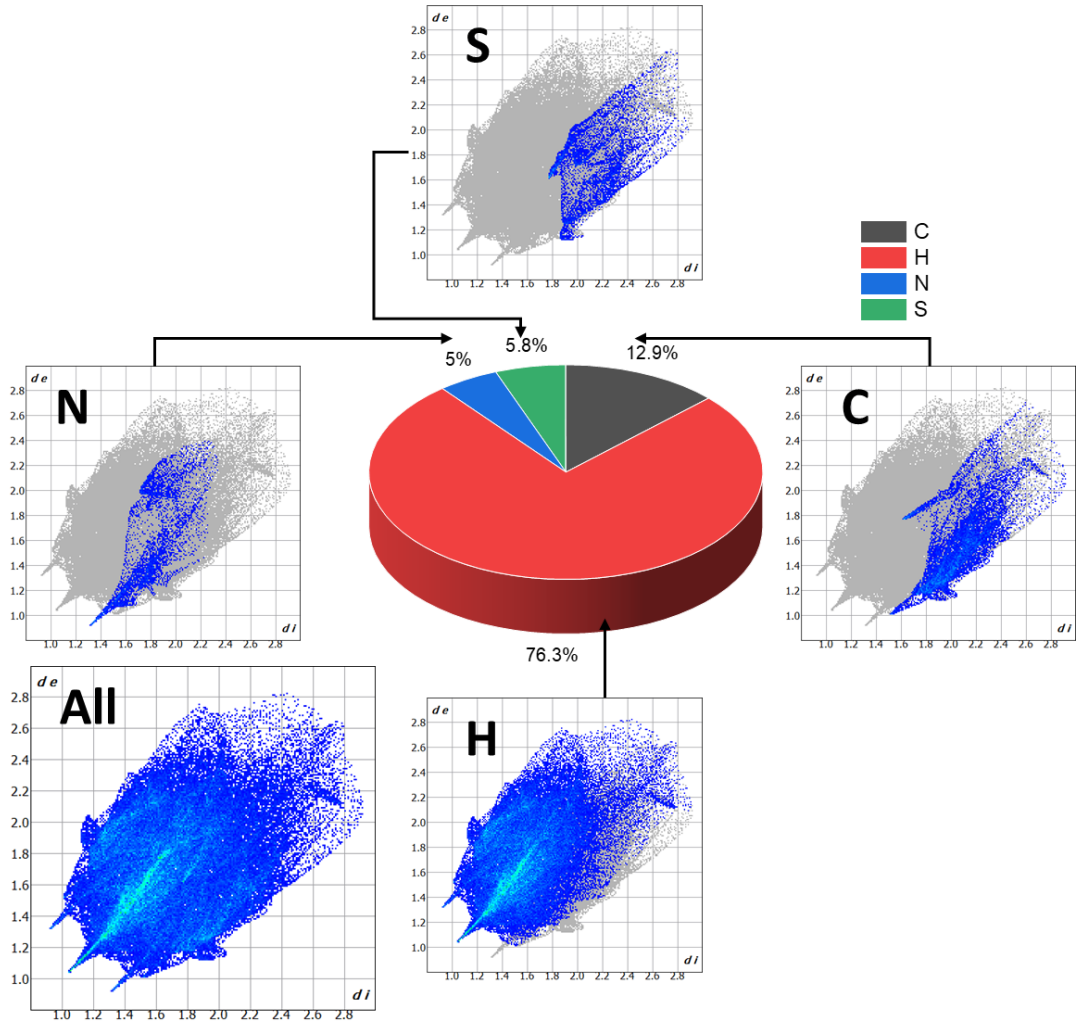

Figure 10. Intermolecular interactions within the molecule and their respective contributions.

Fingerprint analysis results are given in Figure 10. Interactions with contributions constituting less than 1% of the total are excluded from the circular representation. As depicted in Figure 10, the predominant contribution to intermolecular interactions is attributed to H interactions, accounting for 76.3%. The second most substantial contribution is observed in C interactions, representing 12.9%. The remaining interactions comprise 5.8% S and 5% N (Şahin & Dege, 2022).

4. Discussion and Conclusion

We chose Olanzapine ($C_{17}H_{20}N_4S$) as our subject for investigating its theoretical spectroscopic properties. Our quantum chemical analysis of OZ using Density Functional Theory (DFT) has provided valuable insights into its electronic structure and spectrochemical characteristics. Using the B3LYP/LanL2DZ level of basis set was crucial in obtaining the optimized molecular structure, which served as the basis for our calculations. We found that the energy gap between HOMO and LUMO was 3.937 eV, highlighting a significant charge transfer within the molecule. Additionally, bond lengths were calculated using NBO analysis. We conducted FT-IR spectroscopy to gather additional data. The strong FT-IR bands observed at 3074.51 cm^{-1} were attributed to the C1-H24 stretching vibrations of the OZ molecule, while the peak at 1641.87 cm^{-1} in the IR spectra was associated with the N9-C8-C18-C17 stretching vibration.

We also carried out Molecular Electrostatic Potential (MEP) surface analysis, which provided deeper insights into the electrostatic properties of the molecule. Additionally, we reported on the thermal properties of OZ, with thermochemical calculations conducted at a temperature of 298.15 Kelvin and a pressure of 1 atm. The MEP and thermochemical calculations were mutually supportive, providing complementary insights into the electronic properties and thermochemical behavior of OZ. Thermochemical properties were calculated in Gaussian using the DFT method to determine the thermochemical stability of the compound. The total energy is the summation of the total electronic energy and the nuclear-nuclear repulsion. Entropy is a measure of the molecular disorder, or randomness, of a system. Heat capacity, or specific heat, is the heat per unit mass required to raise the temperature by 1°C. The calculations for E (thermal), C_V (heat capacity), and S (entropy) parameters of OZ were obtained and represented graphically as a correlation.

To gain further insights into the structure and interactions of the molecule, we visualized and discussed Hirshfeld surfaces, including parameters like d_i, d_e, d_{norm}, shape index, curvedness, and fragment patches of $C_{17}H_{20}N_4S$. Thus, intermolecular interactions was computed through Hirshfeld surfaces (HS) and two-dimensional (2D) fingerprint plot analysis. Fingerprint analysis results revealed that the most significant contribution to intermolecular interactions was made by hydrogen (H) interactions, accounting for 76.3% of the total. The second-largest contribution came from carbon (C) interactions, at 12.9%, with sulfur (S) and nitrogen (N) interactions making up the remaining 5.8% and 5%, respectively. This comprehensive analysis contributes to our understanding of the behavior and properties of OZ at the molecular level.

To further enhance the research, you might conduct experiments to validate the theoretical results and exploring potential applications of this knowledge in pharmacology or materials science. This could open up new possibilities for understanding the mechanisms of action of the drug or designing novel materials based on the results of its molecular level characterization.

References

Alam, M. S., & Lee, D. U. (2017). Spectral (FT-IR, FT-Raman, UV, and fluorescence), DFT, and solid state interaction analyses of (E)-4-(3, 4-dimethoxybenzylideneamino)-1, 5-dimethyl-2-phenyl-1H-pyrazol-3 (2H)-one. *Journal of Molecular Structure, 1128,* 174-185. https://doi.org/10.1016/j.molstruc.2016.08.048

Al-Otaibi, J. S., Albrycht, P., Mary, Y. S., Mary, Y. S., & Księżopolska-Gocalska, M. (2021). Concentration-dependent SERS profile of olanzapine on silver and silver-gold metallic substrates. *Chemical Papers, 75*, 6059-6072. https://doi.org/10.1007/s11696-021-01783-9

Arulraj, R., Sivakumar, S., Suresh, S., & Anitha, K. (2020). Synthesis, vibrational spectra, DFT calculations, Hirshfeld surface analysis and molecular docking study of 3-chloro-3-methyl-2, 6-diphenylpiperidin-4-one. *Spectrochimica Acta Part A: Molecular and Biomolecular Spectroscopy*, 232, 118166. https://doi.org/10.1016/j.saa.2020.118166

Beck, A. D. (1993). Density-functional thermochemistry. III. The role of exact exchange. *The Journal of Chemical Physics*, *98*(7), 5648-6. https://doi.org/10.1063/1.464913

Bhana, N., Foster, R. H., Olney, R., & Plosker, G. L. (2001). Olanzapine: an updated review of its use in the management of schizophrenia. *Drugs*, *61*(1), 111-161. https://doi.org/10.2165/00003495-200161010-00011

Chiodo, S., Russo, N., & Sicilia, E. (2006). LANL2DZ basis sets recontracted in the framework of density functional theory. *The Journal of Chemical Physics 125*(10). https://doi.org/10.1063/1.2345197.

Cramer, C. J. (2013). *Essentials of computational chemistry: theories and models*. John Wiley & Sons. ISBN: 978-0470091821.

Crystallography Open Database. (Online). Date of access: 29.08.2023. Available: https://www.crystallography.net/cod/search.html

Çakmak, R., Başaran, E., Kaya, S., & Erkan, S. (2022). Synthesis, spectral characterization, chemical reactivity and anticancer behaviors of some novel hydrazone derivatives: Experimental and theoretical insights. *Journal of Molecular Structure*, *1253*, 132224. https://doi.org/10.1016/j.molstruc.2021.132224

Devi, P., Fatma, S., Shukla, S., Kumar, R., Singh, V., & Bishnoi, A. (2018). Synthesis, spectroscopic investigation, molecular docking and DFT studies of novel (2Z, 4Z)-2, 4-bis (4-chlorobenzylidene)-5-oxo-1-phenylpyrrolidine-3-carboxylic acid (BCOPCA). *Heliyon*, *4*(12). https://doi.org/10.1016/j.heliyon.2018.e01009

Eryilmaz, S., Gül, M., Kozak, Z., & Inkaya, E. (2017). The Computational Study on (E)-3-(2-Chlorostyryl)-5, 5-Dimethylcyclohex-2-Enone. *Acta Physica Polonica A*, *132*(3), 738-741. https://doi.org/10.12693/APhysPolA.132.738

Frau, J., Muñoz, F., & Glossman-Mitnik, D. (2017). Application of DFT concepts to the study of the chemical reactivity of some resveratrol derivatives through the assessment of the validity of the "Koopmans in DFT"(KID) procedure. *Journal of Theoretical and Computational Chemistry*, *16*(01), 1750006. https://doi.org/10.1142/S0219633617500067

Fulton, B., & Goa, K. L. (1997). Olanzapine: a review of its pharmacological properties and therapeutic efficacy in the management of schizophrenia and related psychoses. *Drugs*, *53*, 281-298. https://doi.org/10.2165/00003495-199753020-00007

Hay, P. J., & Wadt, W. R. (1985). Ab initio effective core potentials for molecular calculations. Potentials for the transition metal atoms Sc to Hg. *The Journal of Chemical Physics*, *82*(1), 270-283. https://doi.org/10.1063/1.448799

Hirshfeld, F. L. (1977). Bonded-atom fragments for describing molecular charge densities. *Theoretica Chimica Acta*, *44*, 129-138. https://doi.org/10.1007/BF00549096

Jasińska, B., Kędzior, M., Śniegocka, M., Kozioł, A. E., & Wawrzycka-Gorczyca, I. (2009). Investigation of the free volume in olanzapine by PALS. *Physica Status Solidi C*, *6*(11), 2432-2434. https://doi.org/10.1002/pssc.200982110

Kawahata, M., Tominaga, M., Komatsu, R., Hyodo, T., & Yamaguchi, K. (2020). Inclusion crystals of V-shaped host molecules having trialkoxybenzene moieties with a carborane or benzoquinone derivative. *Crystal Engineering Communications*, *22*(44), 7648-7653. https://doi.org/10.1039/D0CE01107J

Kebiroğlu, H., & Ak, F. (2023). Molecular Structure, Geometry Properties, HOMO-LUMO, and MEP Analysis of Acrylic Acid Based on DFT Calculations. *Journal of Physical Chemistry and Functional Materials*, *6*(2), 92-100. https://doi.org/10.54565/jphcfum.1343235

Khanum, G., Fatima, A., Siddiqui, N., Agarwal, D. D., Butcher, R. J., Srivastava, S. K., & Javed, S. (2022). Synthesis, single crystal, characterization and computational study of 2-amino-N-cyclopropyl-5-ethyl-thiophene-3-carboxamide. *Journal of Molecular Structure*, *1250*, 131890. https://doi.org/10.1016/j.molstruc.2021.131890

Marques, M. A., & Gross, E. K. (2004). Time-dependent density functional theory. *Annual Review of Physical Chemistry*, *55*, 427-455. https://doi.org/10.1146/annurev.physchem.55.091602.094449

Ochterski, J. W. (2000). Thermochemistry in gaussian. *Gaussian Inc*, *1*, 1-19.

Ozaki, T., Mikami, K., Toyomaki, A., Hashimoto, N., Ito, Y. M., & Kusumi, I. (2023). Assessment of electroencephalography modification by antipsychotic drugs in patients with schizophrenia

spectrum disorders using frontier orbital theory: A preliminary study. *Neuropsychopharmacology Reports*, *43*(2), 177-187. https://doi.org/10.1002/npr2.12318

Paghandeh, H., & Saeidian, H. (2018). Expedient and click synthesis, spectroscopic characterizations and DFT calculations of novel 1, 5-bis (N-substituted 1, 2, 3–triazole) benzodiazepinedione scaffolds. *Journal of Molecular Structure*, *1157*, 560-566. https://doi.org/10.1016/j.molstruc.2017.12.035

Paghandeh, H., Foumeshi, M. K., & Saeidian, H. (2021). Regioselective synthesis and DFT computational studies of novel β-hydroxy-1, 4-disubstituted-1, 2, 3-triazole-based benzodiazepinediones using click cycloaddition reaction. *Structural Chemistry*, *32*, 1279-1287. https://doi.org/10.1007/s11224-020-01698-3

Reutzel-Edens, S. M., & Bhardwaj, R. M. (2020). Crystal forms in pharmaceutical applications: olanzapine, a gift to crystal chemistry that keeps on giving. *International Union of Crystallography Journal*, *7*(6), 955-964. https://doi.org/10.1107/S2052252520012683

Sevvanthi, S., Muthu, S., Aayisha, S., Ramesh, P., & Raja, M. (2020). Spectroscopic (FT-IR, FT-Raman and UV-Vis), computational (ELF, LOL, NBO, HOMO-LUMO, Fukui, MEP) studies and molecular docking on benzodiazepine derivatives-heterocyclic organic arenes. *Chemical Data Collections*, *30*, 100574. https://doi.org/10.1016/j.cdc.2020.100574

Sheikhi, M., Balali, E., & Lari, H. (2016). Theoretical investigations on molecular structure, NBO, HOMO-LUMO and MEP analysis of two crystal structures of N-(2-benzoyl-phenyl) oxalyl: A DFT study. *Journal of Physical & Theoretical Chemistry*, *13*(2), 155-169.

Sigmaaldrich. (2023). Olanzapine. Date of access: 22.12.2023. Available: https://www.sigmaaldrich.com/TR/en/substance/olanzapine31243132539061

Spackman, M. A., & Jayatilaka, D. (2009). Hirshfeld surface analysis. *Crystal Engineering Communications 11*(1), 19-32. https://doi.org/10.1039/B818330A

Spackman, M. A., & McKinnon, J. J. (2002). Fingerprinting intermolecular interactions in molecular crystals. *Crystal Engineering Communications 4*(66), 378-392. https://doi.org/10.1039/b203191b

Surampudi, A. V. S. D., Rajendrakumar, S., Nanubolu, J. B., Balasubramanian, S., Surov, A. O., Voronin, A. P., & Perlovich, G. L. (2020). Influence of crystal packing on the thermal properties of cocrystals and cocrystal solvates of olanzapine: Insights from computations. *Crystal Engineering Communications*, *22*(39), 6536-6558. https://doi.org/10.1039/D0CE00914H

Şahin, S., & Dege, N. (2022). (E)-N-(3-Chlorophenyl)-1-(5-nitro-2-(piperidin-1-yl) phenyl) methanimine: X-Ray, DFT, ADMET, boiled-egg model, druggability, bioavailabilty, and human cyclophilin D (CypD) inhibitory activity. *Journal of Molecular Structure*, *1250*, 131744. https://doi.org/10.1016/j.molstruc.2021.131744

Tanış, E. (2022a). New optoelectronic material based on biguanide for orange and yellow organic light emitting diode: A combined experimental and theoretical study. *Journal of Molecular Liquids*, *358*, 119161. https://doi.org/10.1016/j.molliq.2022.119161

Tanış, E. (2022b). A study of silicon and germanium-based molecules in terms of solar cell devices performance. *Turkish Journal of Chemistry*, *46*(5), 1607-1619. https://doi.org/10.55730/1300-0527.3464

Tanış, E. (2022c). Study of electronic, optoelectronic and photonic properties of NBB material in solvent environments. *Journal of Electronic Materials*, *51*(9), 4978-4985. https://doi.org/10.1007/s11664-022-09730-4

Tanış, E. (2022d). Optical and photonic properties dependence on HNMB solvents: An emitter molecule for OLEDs. *Optik*, *252*, 168576. https://doi.org/10.1016/j.ijleo.2022.168576

Thakuria, R., & Nangia, A. (2011). Polymorphic form IV of olanzapine. *Acta Crystallographica Section C: Crystal Structure Communications*, *67*(11), o461-o463. https://doi.org/10.1107/S0108270111043952

Ulaş, Y. (2020). Natural bond orbital (NBO) population analysis and non-linear optical (NLO) properties of 2-(azepan-1-yl (naphthalen-1-yl) methyl) phenol. *International Journal of Chemistry and Technology*, *4*(2), 138-145. https://doi.org/10.32571/ijct.751001

Wang, W., Ling, Y., Yang, L. J., Liu, Q. L., Luo, Y. H., & Sun, B. W. (2016). Crystals of 4-(2-benzimidazole)-1, 2, 4-triazole and its hydrate: preparations, crystal structure and Hirshfeld surfaces analysis. *Research on Chemical Intermediates*, *42*, 3157-3168. https://doi.org/10.1007/s11164-015-2203-2